Ionic Shell and Subshell Structures in Aluminum and Gold Nanocontacts

E. Medina, M. Díaz, N. León, C. Guerrero, and A. Hasmy
Centro de Física, Instituto Venezolano de Investigaciones Científicas, Apartado 21827, Caracas 1020A, Venezuela

P. A. Serena
Instituto de Ciencias de Materiales de Madrid, Consejo Superior de Investigaciones Científicas, Cantoblanco, 28049-Madrid, Spain

J. L. Costa-Krämer
Instituto de Microelectrónica de Madrid, Consejo Superior de Investigaciones Científicas, 28760 Tres Cantos, Madrid, Spain
(Received 19 September 2002; published 10 July 2003)

Conductance histograms of aluminum and gold nanocontact rupture are studied experimentally and simulated using embedded atom potentials to assess the interplay between electronic and structural properties at room temperature. Our results reveal a crossover from quantized conductance structures to crystalline faceting or geometric shell/subshell structures at 300 K. The absence of electronic shell structure in gold and aluminum is in stark contrast with the behavior of alkaline metal nanowires which emulate their cluster counterparts. Semiclassical arguments suggest why rapid dominance of ionic structures takes place, and possible nanowire architectures are proposed in consistency with both the experimental and simulated nanocontact data.

DOI: 10.1103/PhysRevLett.91.026802 PACS numbers: 73.40.Jn, 68.37.Ef, 73.23.Ad

Magic shell configurations in clusters [1,2], nanowires, and contacts [3] play an important role in understanding the architecture of materials at the atomic scale. Alkali and noble metal clusters are well described by jellium models where electronic energy fluctuations play a dominant role over ionic crystalline order [1]. Clear evidence of this shell structure is also found for alkali metal contacts through the oscillations observed in conductance histograms obtained during breaking contact experiments [3]. The resulting oscillations in the conductance can be directly associated with geometry dependent semiclassical electron orbits [3,4]. First principle molecular dynamics (MD) simulations [5] have also confirmed the existence of icosahedral packing in breaking nanocontacts similar to those found for clusters.

Nevertheless, there is another class of metallic species—including Al and Pb—which has been controversial, where preferential cluster configurations are not driven by electronic energy fluctuations but by crystal field effects [1,6]. In particular, aluminum clusters represent a notable case since their semiclassical description implies anomalously soft wall electronic potentials [7], whereas Martin [6] demonstrated that its shell behavior could also be explained by the filling of successive triangular facets (ionic subshell structure) of an octahedron.

For sufficiently large structures, the dominance of crystal fields with respect to electronic effects must eventually occur in all metals since bulk crystalline order must prevail. There is then a critical length scale above which lattice ordering energy dominates the electronic contribution. For clusters, according to the Strutinski theory, the fluctuation in the electronic energy contribution varies as $\delta F \sim k_F^2/R^{1/2}$, where k_F is the Fermi wave vector and R is the cluster radius. As the radius of the cluster increases, the energy oscillations decrease so that the ionic energy benefit eventually dominates. For cylindrical-type structures, such as wires and contacts, the semiclassical theory predicts an analogous relation $\delta F \sim k_F^{3/2}/R$ [4]. The stronger decay as $1/R$ of electronic energy oscillations for this geometry determines, in principle, an earlier crossover between electronic and ionic contributions leading to predominant crystalline shell features.

The first experimental evidence of such a crossover in nanowires was reported by Yanson *et al.* [8] for potassium nanowires at 100 K. The experimental crossover radius is about 3–4 atoms, less than half the one noticed for potassium clusters in agreement with the semiclassical argument. For thin wires, the predominance of ionic energy contribution does not imply bulk crystalline order, since surface energy can be dominant. An interesting possibility is the existence of "weird" wire configurations [9], where surface configurations are optimized by close packing hexagonally. Some of the suggested structures have highly nontrivial chiral coiling [9] and have been experimentally observed [10].

In this Letter we report both experimental results and embedded atom MD simulations of oscillations in Au and Al conductance histograms. Experiments support the existence of ionic subshell, facet growing structures in nanocontacts at room temperature. Candidate crystalline structures are discussed, offering good agreement with measured data. MD simulations, accounting mostly for the ionic contribution, offer an excellent account of the experimental data for both Al and Au metals.

The experimental study of the conductance histograms was carried out using a custom-made scanning tunneling microscope able to form and break contacts between two metallic polycrystalline electrodes. Repeated indentation

to form nanocontacts was achieved by a voltage ramp, typically ± 100 V at 1 Hz, fed to a piezoelectric actuator. The current between tip and sample at constant bias voltage was measured at the last stages of the contact rupture using a current-voltage (I-V) converter. The current signal, triggered properly, was digitized and acquired with a Tektronix TDS220 oscilloscope and transferred to a personal computer, where the conductance trace was stored to build the conductance histogram. Au contacts were broken both within 100% neutral paraffinic oil on the electrodes [11] and in high vacuum conditions with 80 mV bias voltage, whereas Al contacts were broken only under high vacuum conditions and 20 mV bias voltage, ensuring cleanliness of Al surfaces with periodic current discharges.

Figure 1 shows the conductance histograms for Au and Al at room temperature. In order to resolve the conductance histogram peak structure, we have evaluated its second derivative $\Delta_2(G)$ smoothing [2] (see the inset of Fig. 1). The observed minima correspond to the more stable configurations of the nanocontact. This method avoids the subtraction of an arbitrary function in order to eliminate the large background inducing a nonuniform shifting of the peaks (indicated by arrows).

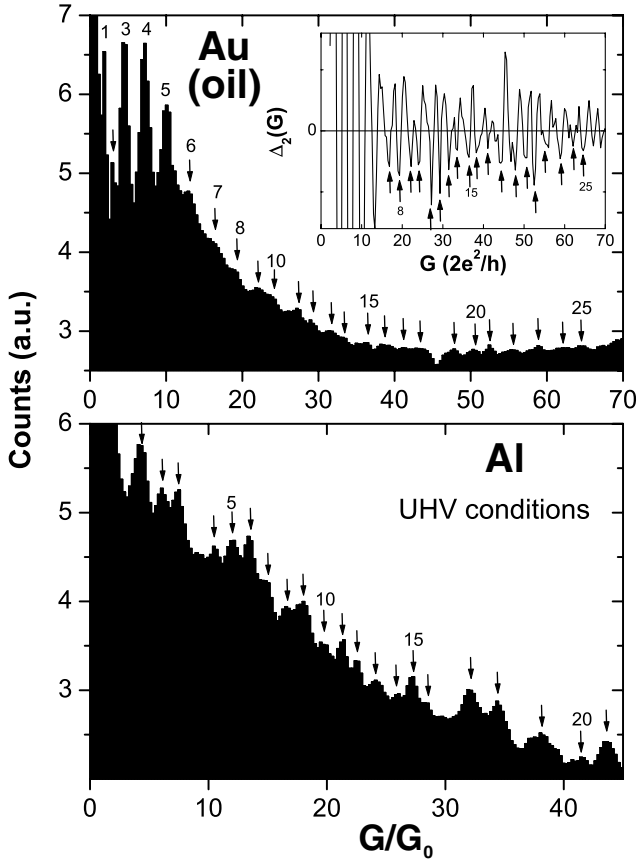

FIG. 1. Experimental conductance histograms for Au in oil, built from 6000 curves, and Al, built from 1073 curves, at room temperature. The inset (for Au) shows the second derivative $\Delta_2(G)$ of the conductance histogram to achieve better resolution of the preferred conductance values. Arrows indicate the set of identified main peaks both in the histogram and in the second derivative.

The conductance of a nanowire is related to its radius through the Sharvin semiclassical formula [12]

$$g = \left(\frac{G}{G_0}\right) = \left(\frac{k_F R}{2}\right)^2 \left(1 - \frac{2}{k_F R} + \ldots\right), \qquad (1)$$

where $G_0 = 2e^2/h$ is the conductance quantum. The presence of a shell structure is revealed by demonstrating a linear relation between R and the peak index number of the oscillating thermodynamic potential determining the stability of the structure [1,4]. Stability, in turn, enhances the probability of occurrence of the particular geometric configuration. Thus, in nanowires these configurations (i.e., cross sections) can be directly monitored by the conductance [3]. From Eq. (1), $g^{1/2} \propto R$, apart from small corrections from the perimeter contribution, so a linear relation of such a quantity versus the peak number in the Au histogram of Fig. 1 indicates the existence of shells. Figure 2 shows $g^{1/2}$ versus the conductance peak number at 300 K for Au. The data points first rise with a slope 0.46 ± 0.01, smaller than that expected for electronic

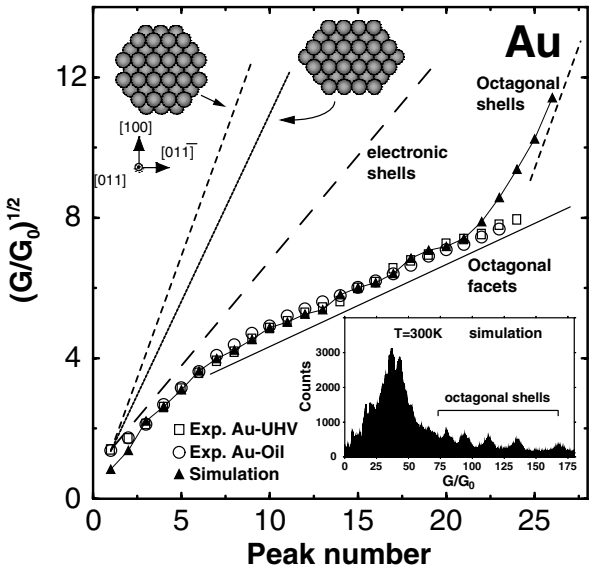

FIG. 2. $(G/G_0)^{1/2}$ versus the peak number for Au in oil (of Fig. 1) and also Au in UHV (2900 curves), as obtained from the experimental histograms (open circles and squares) and the simulation (bold triangles). The top insets illustrate the candidate crystalline structures proposed for the section of the wire corresponding to the full ionic shell slopes (see text). The bottom inset shows the simulated conductance histogram at room temperature indicating the peaks associated with complete octagonal shells. The lines indicate slopes for full octagonal shells (short dashed line), full hexagonal shells (dotted line), electronic shells (long dashed line), and octagonal facets as indicated.

shells (~ 0.59 as reported in Ref. [3]) implying the absence of electronic shells in this low conductance region within the error bars. Beyond the seventh peak, the curve settles onto a linear behavior of slope 0.21 ± 0.02. The initial subelectronic filling behavior seems to follow in part from the succesive occupation of individual quantum modes leading to regular conductance quantization.

It is then clear that the high conductance region must be interpreted in terms of ionic shells. It is expected that more stable configurations will tend to maximize the number of [111] facets although a different wire axis could appear in actual experiments. The inset of Fig. 2 shows two proposed candidate structures for fcc metal nanowires. The first one (following the Wulff-type construction) has a hexagonal cross section with an axis oriented in the [011] direction, and six equal area facets, four of them hexagonally packed. The second energetically favored structure is octagonal[9], also with the axis along the [011] direction but with facets of exposed area fractions β_{ijk}: $\beta_{111} = 0.55$, $\beta_{100} = 0.25$, and $\beta_{110} = 0.20$ accounting for both surface and edge energies.

Growing the cross sections of the proposed wire structures by complete layers of atoms results in a deterministic increase of the nanowire radius. Using Eq. (1), one can compute the conductance $g(m)$ as a function of the number of complete crystalline layers m. The derivative of such an expression leads to a relation for the slope, $\alpha_1 = d(g^{1/2})/dm = 3^{5/6}\pi^{1/6}/2^{13/12} \sim 1.427$ [8] for the hexagonal section. Such a slope is depicted in Fig. 2 and is clearly too high to explain the results. Nevertheless, if facets are filled individually, as previously discussed for Al clusters and suggested by Yanson *et al.*, the slope decreases sixfold, i.e., $\alpha_1/6 \sim 0.24$ in close agreement with the data. The second proposed cross section leads to the slope $\alpha_2 \sim 1.844$, far from the experimental result. However, dividing by eight facets yields $\alpha_2/8 \sim 0.23$, approaching slightly better the measured slope. Although there are small differences in the slopes, the second proposed crystalline section approaches the measured value within the error bars (see the Fig. 2 caption).

Previous works [13,14] have shown that for Au every addition of an atom opens a single channel so the conductance, in units of $2e^2/h$, equals the number of atoms at the nanocontact minimum section. With this fact in mind, we performed MD simulations of breaking Au nanocontacts in order to compute the minimum cross section histograms [15]. A semiempirical embedded atom method has been implemented to describe this metallic system [16]. The method includes many body cohesive effects and has enjoyed a great deal of success describing a wide variety of bulk and surface properties observed experimentally [17,18] as well as nanocontact formation [19,20]. For Au, the embedding function considered is proposed in Ref. [21]. Details of the nanocontact simulations for Al were described in Refs. [15,22].

As a starting point of our MD simulation we consider a parallelepiped supercell containing 3900 atoms with a cross section of 200 atoms, ordered according to a fcc crystallographic structure. Two frozen slabs of atoms at each end are used to pull on the structure (see Ref. [15] for further details). Atoms were initially distributed in layers perpendicular to the (111) direction (wire axis) along which the contact will be elongated until breaking. The resulting minimum cross section histogram (in units of the number of atoms S_N), obtained by accumulating 200 breakage events, is depicted in the bottom inset of Fig. 2. By computing the total neck area cross section $A_n = S_N a_0$, where a_0 is the bulk atomic cross section, one is able to estimate the neck radius $R = (A_n/\pi)^{1/2}$ and therefore the conductance following Eq. (1). Using the same procedure described for the experimental data we plot, in Fig. 2, $(G/G_0)^{1/2}$ versus the peak number for Au. As only the slope of the curve is of direct physical significance (the cut in the abscissa depends on peak numbering), the simulated curve has been shifted upward (by roughly two G_0 units) so a direct comparison with experimental data can be made. Note that the agreement between simulated and experimental slopes is remarkable over a range comprising 20 peaks.

For large diameter wires in the simulations the detailed peak structure observed at intermediate conductance values gives way to broader maxima (see the bottom inset in Fig. 2) which obscure details of the peak structure corresponding to subshells observed in the Au experimental histogram. Remarkably the high slope observed at large conductance values agrees well with that expected for complete shells for the octagonal candidate crystalline structure. Whether this will occur eventually in the experiments, at larger conductances, has not been determined. Such a crossover could be induced in simulations due to the chosen orientation of the frozen slabs used to pull on the dynamic structure, prematurely favoring complete shell filling. Larger simulations taking account of other orientations are in progress.

It has been shown [23,24] that a monoatomic Al contact conducts through three available channels, with a total conductance of approximately G_0. By comparing Al experimental conductance histograms and MD simulations, the work of Díaz *et al.* [20] confirms the close correspondence between conductance and the number of atoms in the wire cross section. Furthermore, at large neck diameters, one can expect that the semiclassical approximation should work well. Aluminum is of particular interest because, for clusters, its preferred structures are always dominated by ionic subshells or faceting. In order to test if the ionic behavior is also present in Al nanocontacts, we built experimental as well as computational conductance (section) histograms. We observe strikingly similar results to those of Au. In Fig. 3 we summarize the Al results. Again, the Al simulated histograms (top inset of the figure) reveal both octagonal

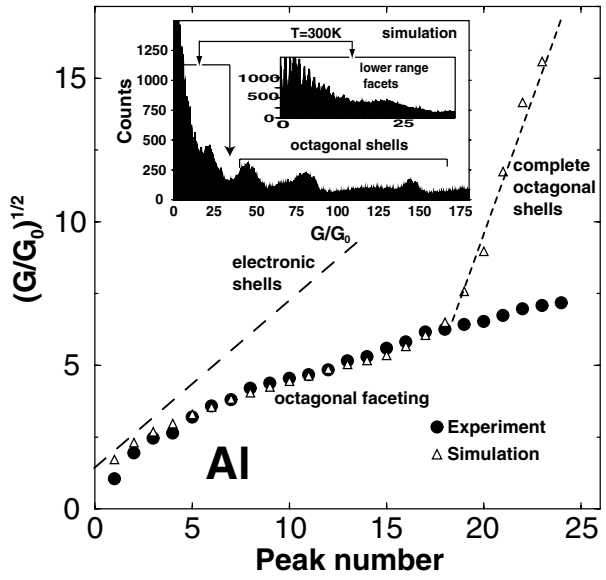

FIG. 3. $(G/G_0)^{1/2}$ versus the peak number for Al in UHV, as obtained from the experimental histogram (black circles) and the simulation (open triangles). The long (short) dashed lines correspond to the expected slopes for electronic shells (complete octagonal shells as proposed in Ref. [9]). The inset shows the corresponding simulation histogram highlighting both the low conductance faceted and the high conductance octagonal shell regimes.

faceting and, at large conductance values, the ionic complete shell structure. The intermediate and even the low conductance value slopes of Al experiments are well recovered by our simulations.

In conclusion, we have presented evidence of ionic shell and subshell structures during nanocontact breakage of Au and Al wires at room temperature. At low conductance values, the formation of stable configurations exhibits a subeletronic filling behavior possibly due to a very early crossover between electronic and ionic shells as argued in the introduction. Thus in Au and Al nanocontacts, electronic shells are not evident. At intermediate conductance values, the experimental and simulated peak number curves evidence a slope approximately equal to 0.2, in good agreement with the expected value for ionic subshell (faceted) formation in fcc geometries. The simulations predict that for large conductance values, details of the subshell formation can be lost in favor of broad maxima consistent with complete ionic shell formation in fcc nanowires [9]. This deviation from the experimental result is clearly not due to the Sharvin approximation used since the semiclassical formula should be better justified for thicker contacts. We believe that it is a result of a bias, produced by the special (111) boundary conditions [15] used, on the nanocontact structure favoring complete shells. We believe that our study consolidates conductance histograms as a new powerful tool for the study of the stable configurations of nanostructures and the determination of the corresponding magic numbers.

We acknowledge P. García-Mochales and J. J. Sáenz for helpful discussions and Cecalcula (Venezuela) for computer facilities. This work has been partially supported by the CSIC-IVIC researchers exchange program and by the Spanish MCyT (Projects No. BFM2000-1470-C02-01 and No. MAT2000-0033-P4-03).

[1] M. Brack, Rev. Mod. Phys. **65**, 677 (1993).
[2] W. A. de Heer, Rev. Mod. Phys. **65**, 611 (1993).
[3] A. I. Yanson, I. K. Yanson, and J. M. van Ruitenbeek, Nature (London) **400**, 144 (1999); Phys. Rev. Lett. **84**, 5832 (2000).
[4] C. Yannouleas, E. N. Bogachek, and U. Landman, Phys. Rev. B **57**, 4872 (1998).
[5] R. N. Barnett and U. Landman, Nature (London) **387**, 788 (1997).
[6] T. P. Martin, U. Naher, and H. Shaber, Chem. Phys. Lett. **199**, 470 (1992).
[7] J. Lermé, M. Pellarin, J. L. Vialle, B. Baguenard, and M. Broyer, Phys. Rev. Lett. **68**, 2818 (1992).
[8] A. I. Yanson, I. K. Yanson, and J. M. van Ruitenbeek, Phys. Rev. Lett. **87**, 216805 (2001).
[9] O. Gülseren, F. Ercolessi, and E. Tosatti, Phys. Rev. Lett. **80**, 3775 (1998); E. Tosatti *et al.*, Science **291**, 288 (2001).
[10] Y. Kondo and K. Takayanagi, Science **289**, 606 (2000).
[11] Oil prevents oxidation of the contact area and has negligible effects, as compared to UHV conditions, on Au and Al conductance histograms. This is shown at low conductance values in M. Díaz *et al.*, Nanotechnology **13**, 43 (2002) and at high conductance values in M. Díaz *et al.*, Nanotechnology **14**, 113 (2003).
[12] A. García-Martin, J. A. Torres, and J. J. Sáenz, Phys. Rev. B **54**, 13 448 (1996).
[13] H. Ohnishi *et al.*, Nature (London) **395**, 780 (1998).
[14] V. Rodrigues *et al.*, Phys. Rev. Lett. **85**, 4124 (2000).
[15] A. Hasmy, E. Medina, and P. A. Serena, Phys. Rev. Lett. **86**, 5574 (2001).
[16] For a review, see M. S. Daw, S. M. Foiles, and M. I. Baskes, Mater. Sci. Rep. **9**, 251 (1993).
[17] B. W. Dodson, Phys. Rev. Lett. **60**, 2288 (1988).
[18] J. C. Hamilton, M. S. Daw, and S. M. Foiles, Phys. Rev. Lett. **74**, 2760 (1995).
[19] U. Landman, W. D. Luedtke, N. Burnham, and R. J. Colton, Science **248**, 454 (1990).
[20] M. Díaz, J. Costa-Krämer, E. Medina, P. A. Serena, and A. Hasmy, Nanotechnology **12**, 118 (2001).
[21] M. I. Haftel, Phys. Rev. B **48**, 2611 (1993).
[22] Y. Mishin *et al.*, Phys. Rev. B **59**, 3393 (1999).
[23] E. Scheer *et al.*, Phys. Rev. Lett. **78**, 3535 (1997); Nature (London) **394**, 154 (1998).
[24] J. C. Cuevas, A. Levy Yeyati, and A. Martin Rodero, Phys. Rev. Lett. **80**, 1066 (1998).